Priority Report

Cancer Research

Macrophage Delivery of an Oncolytic Virus Abolishes Tumor Regrowth and Metastasis after Chemotherapy or Irradiation

Munitta Muthana[1,2], Samuel Rodrigues[2], Yung-Yi Chen[1], Abigail Welford[1], Russell Hughes[1], Simon Tazzyman[1], Magnus Essand[3], Fiona Morrow[2], and Claire E. Lewis[1]

Abstract

Frontline anticancer therapies such as chemotherapy and irradiation often slow tumor growth, but tumor regrowth and spread to distant sites usually occurs after the conclusion of treatment. We recently showed that macrophages could be used to deliver large quantities of a hypoxia-regulated, prostate-specific oncolytic virus (OV) to prostate tumors. In the current study, we show that administration of such OV-armed macrophages 48 hours after chemotherapy (docetaxel) or tumor irradiation abolished the posttreatment regrowth of primary prostate tumors in mice and their spread to the lungs for up to 27 or 40 days, respectively. It also significantly increased the lifespan of tumor-bearing mice compared with those given docetaxel or irradiation alone. These new findings suggest that such a novel, macrophage-based virotherapy could be used to markedly increase the efficacy of chemotherapy and irradiation in patients with prostate cancer. *Cancer Res; 73(2); 490–5. ©2012 AACR.*

Introduction

Solid human and murine tumors often respond well initially to conventional, frontline therapies such as chemotherapy and radiotherapy, leading to the cessation of tumor growth and even tumor shrinkage. However, a major clinical problem is the subsequent regrowth of such tumors—both at the site of the primary tumor and/or distant sites. This relapse results in patients receiving multiple rounds of the same or different therapies.

Monocytes are continually recruited into tumors where they differentiate into tumor-associated macrophages (TAM) and accumulate in poorly vascularized, hypoxic areas (1, 2). We showed previously that macrophages can be used to deliver a hypoxia-regulated, prostate-specific oncolytic virus (OV) to such sites in prostate tumors (3). To do this, macrophages were cotransduced with a hypoxia-regulated E1A/B construct and an E1A-dependent oncolytic adenovirus. The proliferation of the virus was also restricted to prostate tumor cells using prostate-specific promoter elements from the TARP, PSA, and PSMA genes. When such cotransduced cells were injected into tumor-bearing mice, they protected the virus from neutralizing antibodies in the circulation and delivered it to tumors. Once inside hypoxic tumor areas, E1A/B proteins were expressed by the cotransduced macrophage, activating replication of the adenovirus. This was then released and infected neighboring tumor cells in both hypoxic and well-oxygenated areas of tumors, replicated further and lysed each new host cell. This then resulted in the marked inhibition of both primary tumor growth and the formation of pulmonary metastases (3).

Both chemotherapy and tumor irradiation are now known to cause not only the formation of large areas of tumor hypoxia and necrosis (4, 5) but also a marked increase in macrophage recruitment by tumors (6–9). The aim of the current study was to see if this therapy-induced macrophage recruitment could be exploited to deliver a second, potent therapeutic insult to tumors after therapy—large quantities of an oncolytic virus—and, in doing so, markedly increase the efficacy of such standard therapies. Injection of cotransduced macrophages were administered 48 hours after chemotherapy (docetaxel) and tumor irradiation and found to halt both the regrowth and metastatic spread of human prostate tumor xenografts after these therapies.

Materials and Methods

Mouse procedures and human monocyte isolation were conducted in accordance with the University of Sheffield Ethics Committee and UK Home Office Regulations.

Isolation of human monocytes and generation of monocyte-derived macrophages

Macrophages were prepared from mononuclear cells isolated from buffy coats (Blood Transfusion Service; ref. 3).

Authors' Affiliations: [1]Academic Unit of Inflammation & Tumor Targeting, [2]Academic Unit of Rheumatology & University of Sheffield Medical School, Sheffield, United Kingdom; and [3]Department of Immunology, Genetics, Pathology, Uppsala University, Rudbeck Laboratory, Uppsala, Sweden

Note: Supplementary data for this article are available at Cancer Research Online (http://cancerres.aacrjournals.org/).

Corresponding Authors: Claire E. Lewis, Floor E, University of Sheffield Medical School, Beech Hill Road, Sheffield, S10 2RX, UK. Phone: 44-114-2712903; Fax: 44-114-2712903; E-mail: Claire.lewis@sheffield.ac.uk and Munitta Muthana, Floor K, University of Sheffield Medical School, Beech Hill Road, Sheffield, S10 2RX, UK. Phone: 44-114-265852; Fax: 44-114-2713314; E-mail: m.muthana@sheffield.ac.uk

doi: 10.1158/0008-5472.CAN-12-3056

Cotransduction of primary monocyte-derived macrophages

To prevent undesirable viral recombination events, the HRE-regulated E1A/B gene constructs were transferred into macrophages by plasmid transfection rather than coinfection with a second viral vector. For cotransduction, monocyte-derived macrophages (MDM; 2×10^6) that had been cultured for 3 days were infected with adenovirus with a multiplicity of infection (MOI) of 100 plaque-forming unit (PFU)/cell and incubated overnight and then transfected with 5 μg pcDNA3.1(+)-HRE-E1A/B (HRE-E1A/B) construct using the Amaxa Macrophage Nucleofection Kit (Amaxa Biosystems). Optimal transduction of MDMs was determined using a reporter adenovirus (AdCMV-GFP). This was achieved with an MOI of 100 PFU/cell as measured by flow cytometry for expression of GFP (3).

Mice

Male CD1 athymic mice were used in these studies (Charles Rivers). LNCaP:LUC cells were obtained from Professor Magnus Essand (Uppsala, Sweden; ref. 10). The cells were cultured in RPMI-1640 supplemented with 10% FBS in a humidified, 5% CO_2 atmosphere at 37°C. Tumor cells are routinely tested for authenticity by microsatellite genotyping at the ECACC and mycoplasma testing (GENEFLOW).

Orthotopic prostate xenograft model. One million LNCaP-LUC cells were mixed 1:1 in Matrigel and injected into the dorsolateral prostate. Tumor take was monitored by bioluminescence imaging using the IVIS Lumina II imaging system (Caliper Life Sciences). This detects live luciferase-labeled tumor cells, enabling real-time monitoring of tumor growth and spread in the mice. The mice were injected intraperitoneally (i.p.) with 90 mg/kg D-luciferin (Caliper Life Sciences) resolved in sterile water and anaesthetized using 2.5% isoflurane (Abbott Scandinavia AB) in 100% oxygen at 3.5 L/min (for induction) in the anesthesia chamber of the imaging system. Mice were transferred to the dark box and isoflurane was lowered to 1.5%. Images were taken every 3 minutes as a sequence of 10 images for every group of mice, once a week. Automatic contour regions of interest were created, and the tumor sizes (or tumor radiance) were quantified as photons per second per square centimeter per steradian ($ps^{-1}/cm^2/sr^1$). Progression and spread of tumors were evaluated by calculating the tumor radiance values from inoculated mice in each group.

Subcutaneous prostate xenograft model. LNCaP:LUC cells were mixed 1:1 with Matrigel (BD Biosciences) and 2×10^6 injected subcutaneously into the hind flank region. When the tumors reached 4 mm in diameter, mice were given a single dose of irradiation (20 Gy) using an AGO HS X-ray System MP1 (Gulmay Ltd.). Tumor size was determined using calipers.

Docetaxel studies

About 2×10^6 LNCaP-LUC cells were mixed 1:1 in Matrigel and injected into the dorsolateral portion of the prostate gland of male CD1 athymic mice. Tumor take and size was monitored by IVIS Lumina II imaging (IVIS, Caliper Life Sciences). Mice were injected i.p. with 10 mg/kg docetaxel (Sigma-Aldrich), on days 0, 2, 4, 6, or vehicle (EtOH, Tween-20, 5% glucose at volume 1:1:8). On day 8, mice received tail vein injections of either 3 million cotransduced macrophages (Ad[I/PPT-E1A] or reporter AdCMV-GFP at MOI 100 and HRE-E1A/B), 5×10^{10} Ad[I/PPT-E1A] only or vehicle. Animals were sacrificed once tumors reached the maximum volume permitted by UK Home Office Regulations, and 1 hour before sacrifice, mice were injected i.v. with 60 mg/kg pimonidazole hydrochloride (PIMO; a nitroimidazole compound used for detecting hypoxia in tumor sections). Excised tissues including tumors, kidney, liver, lungs, and spleen were embedded in paraffin wax for histologic/immunocytochemical labeling studies.

Irradiation studies

Male CD1 athymic mice (Harlan laboratories) were injected subcutaneously this time with 2×10^6 LNCaP-LUC cells mixed 1:1 with Matrigel (BD Biosciences) into the hind flank region. This was to allow ease of access for tumor irradiation. When tumors reached 4 mm in diameter, mice received a single dose of 20 Gy radiation therapy. Restraining chambers designed to expose only the flank area of mice were used to allow highly localized irradiation of tumors. These s.c. tumors grew quickly and, to comply with UK Home Office Regulations, were removed by day 14 due to their large size. After 48 hours, this was followed by tail vein injection with 100 μL PBS containing either 3 million cotransduced macrophages (Ad[I/PPT-E1A] or reporter AdCMV-GFP at MOI 100 and HRE-E1A/B), 5×10^{10} Ad[I/PPT-E1A] only or PBS alone as described by us previously (3). Tumor size was determined using calipers. Again, animals were sacrificed once tumors reached the maximum permitted volume and tumors/organs were excised and processed as above.

Histology

Five-micrometer paraffin wax sections from tumors and tissue were cut, dewaxed, rehydrated, and stained with hematoxylin and eosin to enable areas of tumor necrosis to be readily visualized using morphologic criteria—reduced cellular density, pale cytoplasm, and pyknotic nuclei or completely disrupted cells, with or without red blood cell infiltration. Hypoxia-bound pimonidazole (PIMO) was detected in tumor sections using Hypoxyprobe-1MAb1, a monoclonal antibody IgG_1 (Millipore). PIMO labeling was then quantified across whole tumor sections using a random point scoring system based on that described by Smith and colleagues (11). Sections were also incubated with specific antibodies for target antigens; CD31 (1:100), F4/80 (1:80; AbD Serotec), human CD68 (Dako) at 1:100 and E1A at 1:50 (Millipore). A biotinylated secondary antibody system was used in conjunction with a streptavidin-conjugated horseradish peroxidase. Peroxidase activity was localized with diaminobenzidine (Vectastain Elite ABC kit, Vector Labs). Metastatic burden was assessed by serial sectioning of formalin-fixed, paraffin-embedded lung tissue whereby the entire lung was sectioned and the number of metastatic foci (>5 cells) was determined on 5 sections taken every 100 μm. Human LNCaP-LUC cells within the lungs were identified by staining with anti-human EpCAM using the immunohistochemical procedure described above. All immune

localization experiments were repeated on multiple tissue sections and included isotype-matched controls for determination of background staining.

For details of plasmid construction, the oncolytic adenovirus used, generation of MDMs, cotransduction of primary MDMs, assessment of tumor necrosis/hypoxia, tumor metastasis and immunolabeling/analysis of CD31, F4/80, CD68, E1A & Ep-CAM in tumor sections, please see the work of Muthana and colleagues (3) and Supplementary File.

Statistical analysis

In most cases, multiple comparisons of groups was conducted by ANOVA followed by the Tukey–Kramer honest significance difference test (GraphPad Software Inc.). All data represent mean values ± SEM and $P < 0.05$ was considered to be significant. Data in Figs. 1–3 are from a single experiment but essentially similar results were achieved when this was repeated.

Results and Discussion

Three intravenous injections of docetaxel significantly ($P < 0.03$) delayed the growth of orthotopic prostate (LNCaP-LUC) tumors until day 14 (i.e., 10 days after the last docetaxel injection; Fig. 1A and Supplementary Fig. S1A) and improved mouse survival (Fig. 1B). However, tumors then regrew over the next 7 days (i.e., between days 14 and 21)—with increased tumor hypoxia and necrosis evident by day 35 (compared with tumors from the "vehicle" group removed by day 14 due to their large size; Supplementary Fig. S1B and S1D), as was a marked tumor infiltration by murine TAMs by day 2, which was still present at day 35 (Fig. 1C). This concurred with our previous pilot studies (data not shown) and confirmed that tumor infiltration by our infused OV-bearing macrophages was likely to take place if they were injected systemically 2 days following the last of the docetaxel injections. So, this time point was selected for a single

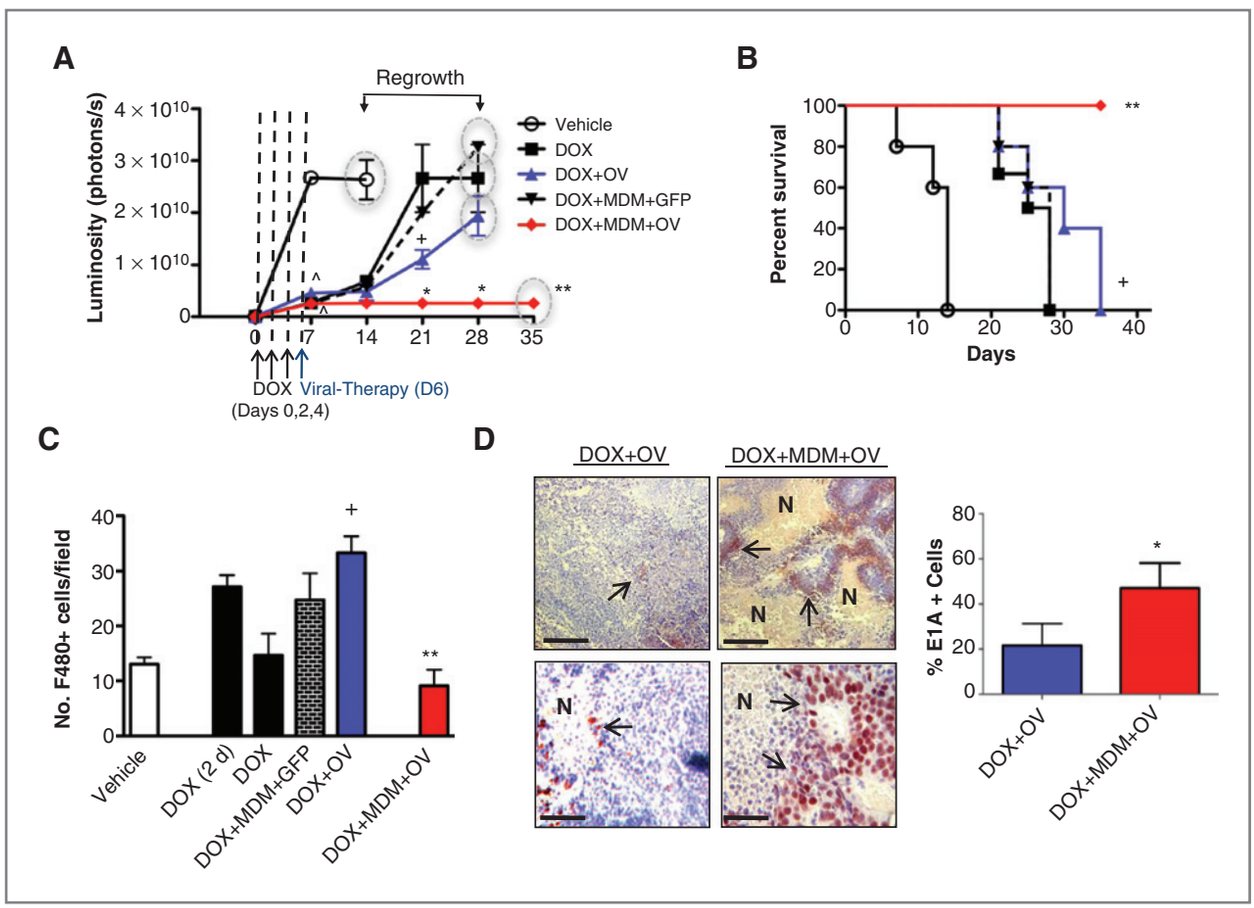

Figure 1. Macrophage delivery of an oncolytic virus (Ad[1/PPT-E1A]) abolishes the regrowth of human prostate (LUC-LNCaP) tumors after treatment with the cytotoxic agent, docetaxel (DOX). Tumor-bearing mice were administered with 3 doses of DOX (10 mg/kg) by i.p. injection on days 0, 2, 4 and then injected i.v, on day 6 with a single dose of either the OV alone or cotransduced MDM. A, tumor luminosity showed that DOX alone prevented tumor growth up to 14 days, but they then rapidly regrew. OV alone delayed this regrowth for up to 7 days, but delivery of the OV via cotransduced MDMs completely abolished it for 35 days. Circles, time points when tumors were taken for analysis. B, mouse survival (NB, the final data points on each line were when mice were culled). C, quantitative analysis of 6 high-power fields (HPF; ×20 magnification) per tissue section from 5 mice per group revealed murine F4/80$^+$ TAMs increased significantly within 2 days of DOX and after injection with DOX + OV. D, OV infection (viral E1A protein staining; red, see arrows) occurred in tumors after DOX + OV alone but was higher in the DOX + cotransduced macrophage group. Representative data shown for 1 of 2 replicate experiments where $n = 5$ mice/group. Data are means ± SEM. Statistical significance differences *, $P < 0.05$; **, $P < 0.01$ compared with DOX + free OV group; $^+$, $P < 0.01$ compared with DOX alone. Bar, 200 μm.

injection of OV-carrying macrophages (and for the purpose of comparison, "free" OV was administered to a separate group). OV alone significantly ($P < 0.01$) delayed tumor regrowth after docetaxel by 7 days (only occurring between days 21 and 28), whereas macrophage delivery of OV completely ($P < 0.0002$) abolished tumor regrowth for up to day 35 and extended the survival of tumor-bearing mice (Fig. 1A and B). Both OV treatments significantly ($P < 0.001$) reduced microvessel density in docetaxel-treated tumors (sampled at day 28 for the docetaxel + free OV group and day 35 for the docetaxel + cotransduced macrophages) compared with docetaxel alone group (at day 28) but failed to affect tumor hypoxia (Supplementary Fig. S1C and S1D). Human $CD68^+$ macrophages were present in tumors in mice injected with either GFP-expressing or OV-bearing macrophages (Supplementary Fig. S1E), and the latter resulted in significantly ($P < 0.001$) more OV detection throughout tumors after docetaxel than in the tumors of mice injected with free OV alone + docetaxel (Fig. 1D).

A single dose of 20 Gy radiotherapy (RT) was also seen to significantly reduced the growth of LNCaP:LUC tumors for 21 days but they then started to regrow and had to be removed at day 35 (i.e., when they reached the tumor size of those in the PBS alone group at day 14). A similar pattern of tumor regrowth occurred in mice receiving RT followed 2 days later by "control" macrophages (i.e., transfected to express the reporter gene, GFP; Fig. 2A and Supplementary Fig. S2A). Thirty-five days after RT, there was a small but insignificant drop in tumor microvessel density compared with that in tumors from the PBS alone group, along with a significant ($P < 0.01$) increase in tumor necrosis and hypoxia in the RT alone group (Supplementary Fig. S2B–S2D). Although these effects in the RT-

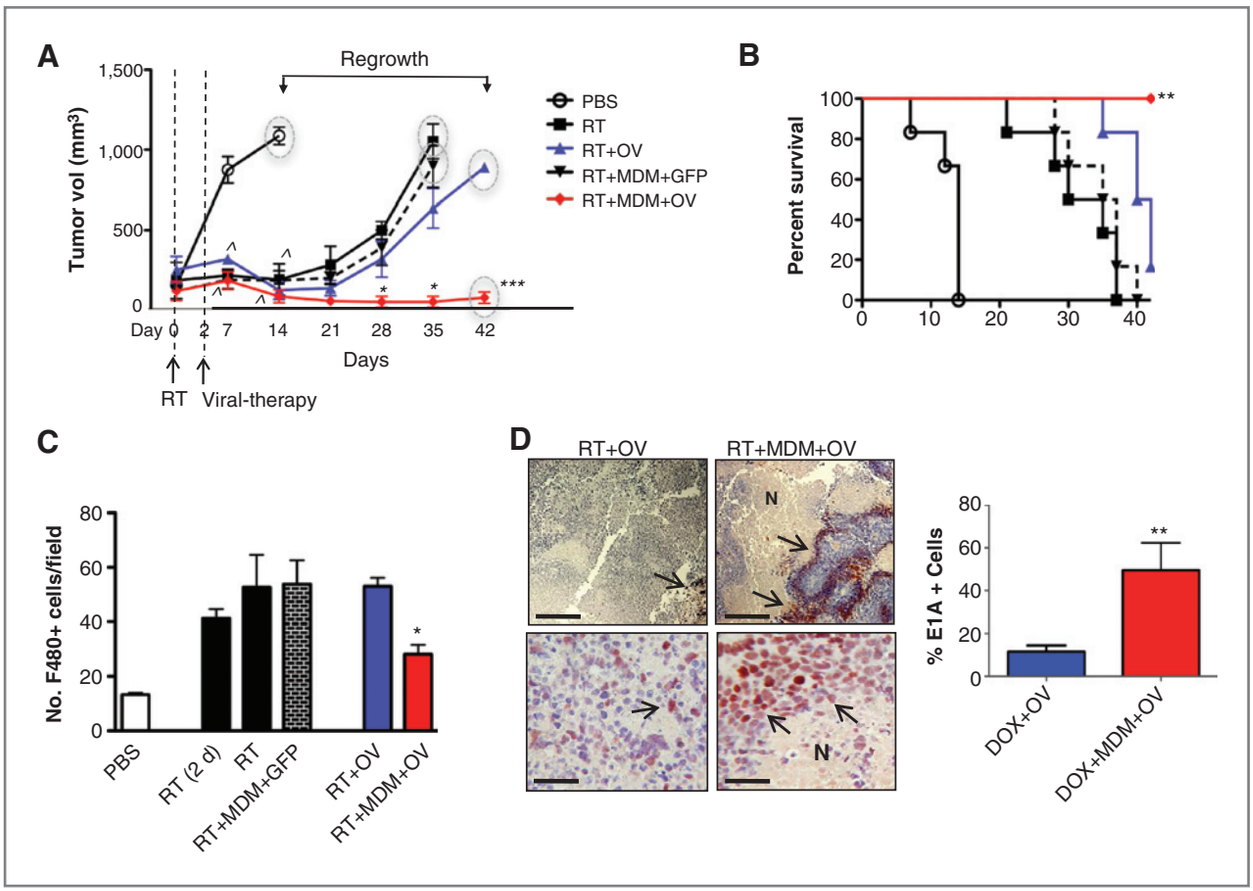

Figure 2. Macrophage delivery of an oncolytic virus (Ad[1/PPT-E1A]) abolishes the regrowth of prostate (LUC-LNCaP) tumors following irradiation. Tumor-bearing mice were administered a single dose of 20 Gy RT and then injected intravenously 2 days later with a single dose of either the oncolytic virus (OV) alone or MDMs cotransduced with an HRE-E1/A/B plasmid and either a reporter virus AdGFP or OV. A, tumor volume showing RT alone significantly reduced tumor growth for 14 days, but tumors then started to regrow by day 21. A single injection of OV alone delayed this post-RT regrowth by up to a week, but viral delivery via cotransduced macrophages completely abolished it for 42 days. Circles represent times when tumors were removed for analysis. B, mouse survival (NB the final data points on each line were when mice were culled). C, the number of murine $F4/80^+$ TAMs in 6 HPF per tissue section increased in all RT-treated groups except the RT + cotransduced macrophage group. D, OV infection (viral E1A protein staining; red, see arrows) occurred in tumors after RT + OV alone but was higher in the RT + cotransduced MDMs group. Representative images of E1A-positive cells at ×10 and ×40 magnification. Representative data shown for 1 of 2 replicate experiments where $n = 6$ mice/group. Data are means ± SEM. Statistical significance differences *, $P < 0.05$; **, $P < 0.01$ compared with RT + free OV group. Bar, 100 μm (×10) and 200 μm (×20).

treated tumors are consistent with those reported for RT in other mouse tumor models (4, 9), it should be noted that they may reflect the effects of tumor regrowth after RT treatment on tumors, rather than RT *per se*.

Two days after RT, a marked tumor infiltration by murine F4/80+ (i.e., host) macrophages occurred and the number of these cells was still elevated at day 35 (Fig. 2C). Again, this concurred with our previous pilot studies (data not shown) and suggested that tumor infiltration by our OV-bearing macrophages would be highly likely to occur if these cells were injected systemically within 2 days of RT. So, as in the docetaxel study, this time point was selected for the single injection of OV-carrying macrophages (or "free" OV). Whereas a single, systemic injection of the latter delayed tumor regrowth after RT by 7 days (so mice could be sacrificed at day 42 rather than 35), OV delivery via cotransduced macrophages significantly extended this, with no regrowth evident by 42 days after RT (i.e., the end of the experiment; Fig. 2A and Supplementary Fig. S2A). This correlated with improved survival rates in the latter group, compared with those receiving RT with free OV (Fig. 2B). There were also significantly ($P < 0.001$) fewer $CD31^+$ blood vessels and more necrosis in tumors receiving macrophage-delivered OV than OV alone (Supplementary Fig. S2B–S2D). Following RT, human $CD68^+$ macrophages were present in tumors receiving macrophage-delivered GFP and OV (Fig. 2C and Supplementary Fig. S2E), leading to widespread expression of OV in the latter group (Fig. 2D).

We next determined how these therapies influenced the development of pulmonary metastases. Few metastases were detected in mice injected with PBS alone (no docetaxel) because, as mentioned previously, primary tumors in this group had to be removed by day 14 (due to their size). Therefore, it was not valid to compare metastases in this control group with the 4 experimental groups. Metastases form in the lungs by day 21 in the LNCaP model used in these studies (Fig. 3A). The formation of lung metastases after docetaxel was abolished when OV-bearing macrophages were injected 2 days after the final docetaxel was delivered (a phenomenon not seen when mice were injected with free OV or macrophages bearing a control, GFP-expressing adenovirus; Fig. 3A and B). OV was detected in some areas of lung in mice injected with OV-bearing macrophages after docetaxel but not docetaxel + free OV (Supplementary Fig. S4A). Similarly, pulmonary metastases were significantly

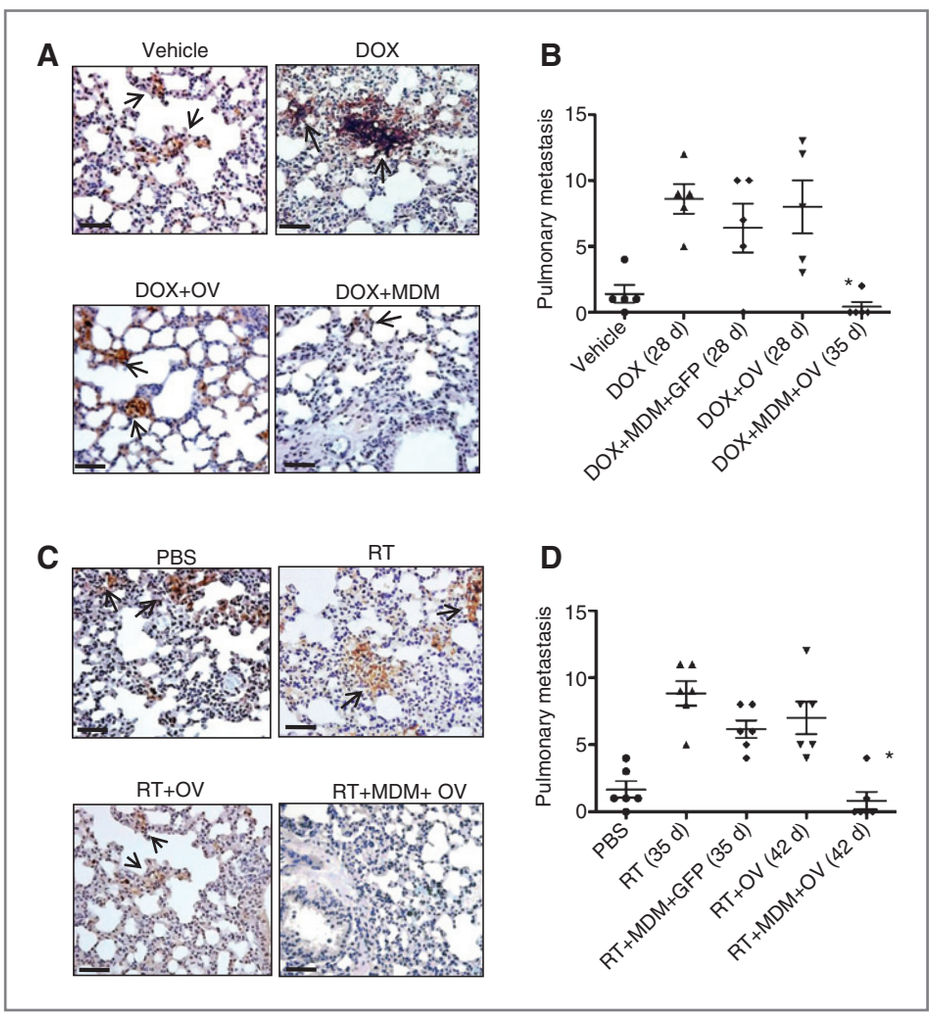

Figure 3. Macrophage delivery of an oncolytic virus (Ad[1/PPT-E1A]) abolishes the formation of pulmonary metastases in mice bearing human prostate (LNCaP-LUC) tumors after docetaxel (DOX) treatment or irradiation. Representative appearance of pulmonary metastases in anti-EpCAM–stained sections revealed very few metastases in the lungs of control tumor-bearing mice by day 14 but were evident by days 28 to 35 in tumors from mice receiving 3 injections of DOX (A and B) or days 35 to 42 in those receiving 20 Gy RT (C and D). Quantification of metastatic foci per lung section per mouse after DOX (B) or RT (D) treatment was not affected by injection of OV alone but was virtually abolished by a single injection of OV-bearing macrophages. Of note, each lung was serially sectioned; 5 sections that were 100 μm apart were stained with anti-EpCAM, and the total number of metastatic foci (>5 cells) was quantified per mouse ($n \geq 5$–6 mice per group). Representative data are shown for 1 of 2 replicate experiments. SEMs are depicted with *, $P < 0.01$ compared with DOX + free OV or RT + free OV groups (as appropriate). Bar, 200 μm.

($P < 0.0012$) higher in mice receiving RT + free OV than in RT + cotransduced macrophages (a valid comparison as both groups were sacrificed on day 42; Fig. 3C and D). OV (E1A staining) was detected in some small areas of the lungs of mice injected with OV-bearing macrophages after RT but not in mice injected with free OV after RT (Supplementary Fig. S4B). In addition to targeting the primary tumor, we believe that our macrophage-based therapy homed to pulmonary metastases and prevented their development.

The use of athymic (nude) mice in the above xenograft tumor model meant we could not assess the immune response of host mice to our cotransduced, human macrophages, immunocompetent mice could not be used because murine cells, including macrophages, do not support adenoviral replication. For this reason, we decided to use a well-characterized human prostate xenograft model rather than a transgenic mouse tumor model (orthotopic in the case of the docetaxel study). It should be noted that the majority of preclinical studies of anticancer gene therapies have used similar human tumor xenograft models (12, 13).

In sum, the current study shows that it is possible to exploit the increased macrophage infiltration in tumors that occurs after chemotherapy or irradiation to deliver a macrophage-based OV therapy. This profoundly suppressed the regrowth and metastatic spread of human prostate tumor xenografts after such frontline therapies. Further studies are now warranted to see if such a combined therapeutic approach will be equally effective in patients with prostate cancer.

Disclosure of Potential Conflicts of Interest

No potential conflicts of interest were disclosed.

Authors' Contributions

Conception and design: M. Muthana, Y.-Y. Chen, C.E. Lewis
Development of methodology: M. Muthana, Y.-Y. Chen, F. Morrow, C.E. Lewis
Acquisition of data (provided animals, acquired and managed patients, provided facilities, etc.): M. Muthana, S. Rodrigues, Y.-Y. Chen, R. Hughes, S. Tazzyman
Analysis and interpretation of data (e.g., statistical analysis, biostatistics, computational analysis): M. Muthana, Y.-Y. Chen, A. Welford
Writing, review, and/or revision of the manuscript: M. Muthana, Y.-Y. Chen, C.E. Lewis
Administrative, technical, or material support (i.e., reporting or organizing data, constructing databases): M. Essand, F. Morrow
Study supervision: M. Muthana, Y.-Y. Chen, C.E. Lewis
Developed and produced the oncolytic virus used in the study and the luciferase-expressing target cell line: M. Essand
Conducted the staining and support practical work, analysis of images, and preparation of macrophages and virus: F. Morrow

Grant Support

Financial support for this project was provided by the Prostate Cancer Charity and Yorkshire Cancer Research.

Received August 2, 2012; revised October 19, 2012; accepted November 10, 2012; published OnlineFirst November 20, 2012.

References

1. Leek RD, Landers RJ, Harris AL, Lewis CE. Necrosis correlates with high vascular density and focal macrophage infiltration in invasive carcinoma of the breast. Br J Cancer 1999;79:991–5.
2. Burke B, Giannoudis A, Corke KP, Gill D, Wells M, Ziegler-Heitbrock L, et al. Hypoxia-induced gene expression in human macrophages: implications for ischemic tissues and hypoxia-regulated gene therapy. Am J Pathol 2003;163:1233–43.
3. Muthana M, Giannoudis A, Scott SD, Fang HY, Coffelt SB, Morrow FJ, et al. Use of macrophages to target therapeutic adenovirus to human prostate tumors. Cancer Res 2011;71:1805–15.
4. Chen FH, Chiang CS, Wang CC, Tsai CS, Jung SM, Lee CC, et al. Radiotherapy decreases vascular density and causes hypoxia with macrophage aggregation in TRAMP-C1 prostate tumors. Clin Cancer Res 2009;15:1721–9.
5. Teicher BA, Holden SA, Ara G, Dupuis NP, Goff D. Restoration of tumor oxygenation after cytotoxic therapy by a perflubron emulsion/carbogen breathing. Cancer J Sci Am 1995;1:43–8.
6. Denardo DG, Brennan DJ, Rexhepaj E, Ruffell B, Shiao SL, Madden SF, et al. Leukocyte complexity predicts breast cancer survival and functionally regulates response to chemotherapy. Cancer Discov 2011;1:54–67.
7. Shree T, Olson OC, Elie BT, Kester JC, Garfall AL, Simpson K, et al. Macrophages and cathepsin proteases blunt chemotherapeutic response in breast cancer. Genes Dev 2011;25:2465–79.
8. He J, Luster TA, Thorpe PE. Radiation-enhanced vascular targeting of human lung cancers in mice with a monoclonal antibody that binds anionic phospholipids. Clin Cancer Res 2007;13:5211–8.
9. Kioi M, Vogel H, Schultz G, Hoffman RM, Harsh GR, Brown JM. Inhibition of vasculogenesis, but not angiogenesis, prevents the recurrence of glioblastoma after irradiation in mice. J Clin Invest 2010;120:694–705.
10. Danielsson A, Dzojic H, Nilsson B, Essand M. Increased therapeutic efficacy of the prostate-specific oncolytic adenovirus Ad[l/PPT-E1A] by reduction of the insulator size and introduction of the full-length E3 region. Cancer Gene Ther 2008;15:203–13.
11. Smith KA, Hill SA, Begg AC, Denekamp J. Validation of the fluorescent dye Hoechst 33342 as a vascular space marker in tumours. Br J Cancer 1988;57:247–53.
12. Fernandes MS, Gomes EM, Butcher LD, Hernandez-Alcoceba R, Chang D, Kansopon J, et al. Growth inhibition of human multiple myeloma cells by an oncolytic adenovirus carrying the CD40 ligand transgene. Clin Cancer Res 2009;15:4847–56.
13. Zhang L, Giraudo E, Hoffman JA, Hanahan D, Ruoslahti E. Lymphatic zip codes in premalignant lesions and tumors. Cancer Res 2006;66:5696–706.